DARYL WASDEN
PAUL BEARD
FINAL REPORT

ABSTRACT

A design of a wireless communication system for a cardiac pacemaker. The processes conducted during a series of experiments culminated in the design of a system that can wirelessly communicate with the pacemaker implanted in human tissue. The system comprises: a transmitter, adapted to serve as a simulated pacemaker and is configured to transmit an electrical signal; a receiver, configured to receive an electric signal from the transmitter; and a personal computer electrically coupled to the receiver and adapted to display medical data pertaining to a patient. The experiments included: 1) the measurement of dielectric properties of materials that simulant human tissue to determine power signal attenuation as it leaves the human body; 2) the measurement of transmission line parameters to evaluate loss of power in the lines; 3) the design of a single-stub matching network to eliminate impedance mismatches between lines, ensuring maximum power transfer to the receiver; 4) the use of numerical analysis and computer program to calculate/observe how magnetic field intensity changes with distance from a power source, as well as predict the future behaviour of an electric signal propagating through materials over time; 6) and an actual prototype design of a frequency shift keying system that enables the transmitter generate enough power to wirelessly communicate data to the receiver. Modeling the system will show how such system can be employed will effectively monitor the health of patients.

missing 5)

EXECUTIVE SUMMARY

The objective of the experiment was to apply transmission-line and electromagnetic theory to design a wireless communication system for an implantable cardiac pacemaker. Ideally, the system will enable real-time wireless transmission of medical data pertaining to the condition of a person's heart and associated organs to an external receiver. This will enable end users, such as medical personnel, to receive the data through a computer screen so that the health of patients using the pacemakers can be continuously monitored. Ultimately, this will help users to quickly respond to any acute heart conditions, preventing the outbreak of major heart problems such as heart failure, heart attacks, etc... To achieve the system design, six progressive experiments were conducted.

The experiments began with the measurements of the dielectric properties of simulant human tissue (e.g., meat, oil, pudding, salt water). The measured values were compared against that of body tissues (e.g., skin, muscle, fat) documented a Final Technical Report [7] and an article, "The Dielectric Properties of Biological Tissues II" [8] to ensure the materials are representative simulant tissues. It was observed that less power penetrates through the simulant tissue as conductivity and signal frequency increases. Using an insulator and a lower frequency signal will maximize penetration of power. Other factors may also affect attenuation like bone, internal reflections, etc... It is recommended that these factors be evaluated before the pacemaker is ready for implantation into a person.

After gaining knowledge about dielectric properties of materials and its effect on power attenuation, a computer program, a capacitance meter, and a time-domain reflectometer were collectively used to measure and calculate important transmission line (e.g., coaxial cable, wires) parameters. The parameters include, but are not limited to: resistance per unit length of line, conductance per unit length of line. With these parameters known, the power attenuation and phase of an electric signal propagating in the line can be calculated.

With this understanding of transmission line characteristics, a single-stub matching network was designed and implemented as part of the receiver. The network included a receiving (monopole) antenna that needed to be designed such that any reactance in the antenna would be eliminated, thus allowing maximum power reception at the receiver. This is vital to minimize the loss of critical medical information that is transmitted from the pacemaker to the receiver where medical personnel can access the data.

The fourth and fifth stages of the experiment involved the application of numerical analysis and the use of a computer programming tools to calculate how magnetic field intensity, generated by the electrical signal, changes with distance as the signal propagates away from its power source. It was concluded that magnetic field intensity decreases linearly with increasing distance. The same tools were used to predict changes in the behaviour of an electrical signal as it propagates through space over time. These simulations demonstrated the power attenuation as a function of the dielectric properties of the human tissue simulant. This has an effect on how far we can implant the cardiac pacemaker and how much power is required for transmission through a person's body.

During the sixth and final stage of the experiment, the results and findings from the previous experiments were used to design an actual prototype of a frequency shift keying (FSK) communication system. The transmitter and receiver were coupled together and a message in Morse code was transmitted to verify the correct functioning of the transmitter in simulant to an external receiver. The successful transmission of the code verified that the prototype system worked.

Spend more time on Conclusion & Recommendations

1.0 INTRODUCTION:

Six lab experiments were conducted in order to design, construct, and test a communication system for the implementation of wireless communications with an implantable cardiac pacemaker. The first experiment involved the measurement of dielectric properties of different materials and how it related to the attenuation of electromagnetic (EM) signal propagation. The second experiment involved the evaluation of signal loss in transmission lines (TL) due to multiple wave reflections caused by impedance mismatches in the TLs. The third experiment involved construction of a single-stub matching network. Matching the load impedance of the antenna to the line maximizes power transfer to the receiver. The fourth experiment involved application of numerical analysis, particularly finite-difference-time-domain (FDTD) methods, to achieve close approximation calculations of magnitudes of EM signals and evaluate the present and future behaviour of EM signals propagating in various mediums. The fifth experiment again involved the application of numerical analysis use of a matrix library (MATLAB) computer program to understand how an EM wave attenuates with distance from an electrical source (e.g., current distribution). Finally, a frequency shift keying (FSK) system was designed, tested, and implemented to operate according to a power link budget, such that a transmitter would transmit enough power to a receiver with minimal loss. Sufficient power is needed so that transmitted information can be available at the receiver for access by an end-user.

The dielectric constant of a material impacts the attenuation of power transmission. Several types of materials were examined, and their dielectric constants were measured using a network analyzer. These materials were beef, oil, a 5% saline solution, and a mixture consisting of instant pudding mix and water. Each material relates to tissues in the human body. When transmitting a signal from within the human body to communicate with something at the surface, the attenuation of biological tissues is the dominant source of power loss. The power loss for 2/3 muscle mass and brain tissue was calculated and plotted to gain a visual understanding of the attenuation occurring in the human body, and it impacted the communication range of the system and the safety of the patient.

The purpose of this experiment was to apply transmission line and electromagnetic concepts in the design of a communications system that would be beneficial to the medical industry. Particularly, what is needed is a system that can wirelessly communicate with an implantable pacemaker inside of a human body. Ideally, the pacemaker can be employed to transmit real-time medical information to a receiver external to the body such that a user may continuously monitor the health of patient(s) from a PC and provide the appropriate medical attention and treatment to them in case of any health issues.

You touch on each experiment in the first paragraph, which is good.
Then it appears the second paragraph relates to lab 1 and no others
Try to avoid this undue emphasis on one lab.
Expand the third paragraph a little more, especially the problems of interest"

2.0 METHODS

2.1 Dielectric Properties of Materials (Lab 1)

A HP-85070M Dielectric Probe Measurement System was used to measure the dielectric constants of beef, oil, 5% saline solution, and a pudding mixture per the lab procedures [1]. The dielectric probe was connected to a HP-8720 Network Analyzer. Before measuring any of the materials, the probe needed to be calibrated. This is done by selecting the "calibration-set frequency" option from the menu of an 85070.exe program available on a desktop computer. To calibrate: first, the dielectric constant of air was measured (an open-circuited load), then a short-circuited load, then distilled water.

Once the system was calibrated, a probe was pressed onto beef, and measurements were taken using the 85070.exe program and the network analyzer. Signals operating at frequencies of 200MHz, 440MHz and 920MHz, respectively, were generated and used to test dielectric properties of the materials. The same procedure was used for the oil, 5% saline solution, and the pudding mixture. The network analyzer read out the values e' and e". These values are not the same as ϵ' and ϵ'' used to describe the dielectric constant of a material. They are related by (1) and (2).

$$\varepsilon' = e'\varepsilon_0 \tag{1}$$

$$\varepsilon'' = \frac{e''}{e'\dot{\varepsilon}'} \tag{2}$$

These values of ϵ' and ϵ'' were used to calculate the attenuation constant using (3) below. Then, assuming low-loss, (3) was used to calculate the attenuation constant and (4) was used to calculate the phase constant. The attenuation constants were compared to measured constants.

$$\alpha=\omega\left\{\frac{\mu\varepsilon'}{2}\left[\sqrt{1+\left(\frac{\varepsilon''}{\varepsilon'}\right)^2}-1\right]\right\}^{1/2} \text{ (Np/m)} \tag{3}$$

$$\varepsilon'=\varepsilon_r\varepsilon_0, \quad \varepsilon''=\sigma/\omega, \quad \mu=\mu_r\mu_0, \quad \omega=2\pi F$$

$$\beta=\omega\left\{\frac{\mu\varepsilon'}{2}\left[\sqrt{1+\left(\frac{\varepsilon''}{\varepsilon'}\right)^2}+1\right]\right\}^{1/2} \tag{4}$$

In order to measure the attenuation constant directly, a probe was connected to the analyzer, on port 1. A folded dipole antenna was placed in a tank of water, acting as a transmitting antenna. An adjustable reference dipole antenna was also connected to the same analyzer, but on port 2. It was placed outside the tank of water in the air, near to the edge of the tank. Measurements of power were taken in decibels for several distances ranging from 3 cm to 10 cm, as listed in Section 3.0, Table 2. After taking the measurements, the values were recorded and applied to (1). The same values were applied to the phase constant equation in (4).

2.2 Transmission Line (TL) Losses (Lab 2)

Per the lab procedures [2], several methods were implemented to calculate/measure parameters of TLs (e.g., coaxial, twin-lead wires). The first method involved writing a MATLAB program to calculate the following parameters of interest: resistance/meter (R'), inductance/meter (L'), conductance/meter (G'), capacitance/meter (C'), attenuation constant (α), phase constant (β), and propagation velocity (Vp).

The parameters values used to determine the effect of each TL on power loss are listed in Section 3.0, Table 3. The MATLAB source code is documented in the lab notebooks.

Another method of measuring TL parameters was the use of a HP 4262A Capacitance Meter. The meter aided measuring the capacitance of a plurality of twin-lead cables (in air), having different dimensions. Then the cables were submerged in sand, and the capacitance of the cables was measured again. After carefully measuring the length of each line, the capacitance per meter (C') values were documented in Section 3.0, Table 4 and compared to the calculated values listed in Table 5, same section.

A 20/20 Time Domain Reflectometer (TDR) was a tertiary way of measuring the TL parameters. The TDR was first calibrated. The TDR was configured to transmit impulse signals through a TL and measure the response (e.g., amplitude, type, and number of wave reflections) of the TLs and terminations to the input signal. The TDR had the capability to display the wave reflections, and export numerical values of the reflections into MS Excel for easy plotting and extraction. After plotting the waveforms for each TL set-up, the graphs were compared to the hand-drawn bounce diagrams completed during pre-lab for further validation.

Another goal of this project was to better understand how the resistance per meter (R') of a long piece of coaxial line differs from its characteristic impedance (Z_0). To accomplish this, a long piece of RG58 coaxial line was measured with a standard digital ohmmeter to obtain the value of R'. Knowing that the characteristic impedance of the line was 50Ω, it quickly became clear that the value of R' is not equivalent to Z_0. Differences between these two characteristics are discussed further in section 4.0.

Another comparison that was made during the course of this project was that of the load reflection coefficients (Γ_L). After drawing/using bounce diagrams to calculate the values of Γ_L, the values were compared with the TDR data values that were plotted on a MS Excel spreadsheet by using (5):

$$\Gamma_L = \frac{Z_L - Z_0}{Z_L + Z_0} \tag{5}$$

Overall, the functionality of the equipment was fine. However, it was observed that the second antenna was very sensitive. For example, the transmitting antenna had to be positioned almost perfectly parallel to the receiving antenna in order to get a smooth wave on the network analyzer screen and a good wave power amplitude measurement. If the antennas were slightly misaligned, a noisy wave with fluctuating values of power amplitude was measured.

2.3 Antennas and Matching (Lab 3)

A HP8720C Network Analyzer was calibrated and employed to measure the impedance of a monopole antenna coupled to one end of a microstrip TL, at a frequency of 440MHz according to the lab procedures [3]. Calibrating the analyzer was a very important step prior to taking any measurements, as it ensured the analyzer was measuring the right electronic devices. In addition, the calibration process lets the analyzer know exactly what it is measuring. Parameters from previous experiments could have been calibrated into the analyzer, resulting in incorrect measurements for the current design being tested. After calibrating the analyzer, dimensions of a 50Ω coaxial cable were measured, as shown in Section 3.0, Table 4.

Next, a very narrow copper wire was employed to build a quarter-wave monopole antenna. The ends of the wire needed to be sanded down to remove the varnish coating the wire, allowing a continuity path. If this is not done the signal may not reach the network. Then, the "port extensions" option in the analyzer was activated. This enabled the power from the analyzer to be delivered through the 50Ω coax and microstrip lines to the antenna, so that the impedance of the antenna can be directly measured. Once this was accomplished, the "port extensions" option was deactivated. The port extensions are used so the length of copper microstrip line will not be added to the length of the antenna and consequently introduce error into the measurements.

More, a microstrip stub having an optimal length was built and placed substantially normal to the line coupled to the antenna to aid in designing a matched network. The objective was to tune the antenna at 440MHz by reducing the length of the antenna such that any reactive impedance of the antenna was eliminated. Despite trimming the monopole antenna to a desirable length (~ 17.5 cm) to eliminate the reactive load impedance of the antenna, the antenna's impedance was measured by the analyzer and the TDR-generated Smith Chart, shown in Section 3.0, Figure 6, indicated the antenna having a small reactive impedance of j4.95 Ω vs. a real impedance of 36Ω as ideally desired. Possible sources for error in these results may be attributed to: the antenna being bent in various points thereon; measurements taken in close proximity to the analyzer; the non-ideal match which resulted in j4.95 Ω impedance difference from the ideal case, internal impedances of the equipment itself.

The single stub matching network is then added to the substrate. The single stub is a piece of copper tape that is cut to the length calculated from the pre-lab. An eraser of a pencil is used to push the stub around on the substrate to eliminate any conductive path. The stub's distance from the antenna and its length are listed in Section 3.0, Table 6.

Further, the magnitude of the reflection coefficient (S11) was measured at 420, 440, and 460 MHz and recorded in Section 3.0, Table 7 and plotted on the analyzer's Smith Chart, as illustrated in Figure 6, same section. The power reflected back to the generator was calculated. Then the accuracy of the match was investigated by viewing the Smith Chart option and observing how close the marker was to the center of the Smith Chart indicating a perfect match.

2.4 Frequency Shift Keying (FSK) System (Lab 6)

In accordance with the lab procedures [6], an E4438C Vector Signal Generator was employed to generate an input signal through a previously constructed circuit comprising a transmitter and receiver, as shown in Figures 13-16. A ZESC-2-11 Power Splitter was coupled to the receiver, enabling two signals to be generated and operated at 420MHz and 460MHz frequencies, respectively. The sensitivity of the receiver was continuously measured until the receiver could no longer receive a signal reliably. A power of -13dBm was observed. Then a voltage controlled oscillator (VCO) was connected to a DC power supply. The voltage was adjusted until the VCO produced frequencies of 420MHz or 460 MHz. The power and frequency was measured, as shown in Section 3.0, Table 9.

Next, an HP-8720, 2-Port Network Analyzer was calibrated and used to measure the reflection coefficient of the receiver and the transmission coefficient of the transmitter (in air and simulant) at 420MHz, 440MHz and 460MHz frequencies. The values of said coefficients are listed in Section 3.0, Tables 9 and 10, respectfully. The transmitter was connected to the network analyzer to port 1 of the analyzer; the receiving antenna was connected to port 2.

Further, an Agilent E4404 ESA-E Series Spectrum Analyzer was used to observe the frequency spectrum of the 420MHz and 460MHz signals. Due to the amplified signal, the power gain at the receiver increased significantly, allowing the signals to be detected 6 times the distance as without the amplifier.

Leveraging MATLAB, a power link budget was calculated and tested for the cardiac pacemaker implantable communication system. A sugary solution was used as simulant for the biological tissue. The dielectric constant of the solution is approximately equivalent to 2/3 muscle. The power link budget program was accurate in calculating the distances at which the receiver could successfully operate. Reflection coefficients, transmission line equations, and plane wave propagation equations were used to calculate the power required for successful transmission. The MATLAB code for the power link budget is documented in the lab notebooks.

A complete communication system was constructed, as shown in Section 3.0, Figures 10 and 11. A signal encoded in Morse Code was sent through the air to verify that wireless communication was possible between the transmitter and receiver. A maximum distance between the transmitter and receiver was measured to determine how far the receiver could be away from the transmitter and still receive a reliable signal, as shown in Section 3.0, Table 11. The same procedure was followed after coupling an amplifier to the receiver. The procedure was not conducted using two amplifiers per the lab instructor. Table 11 shows the maximum distances in which a good signal can be received.

3.0 RESULTS:

As shown in Table 1 below, dielectric properties of materials were measured with the aid of the network analyzer, at 200MHz, 440MHz, 915 MHz, and 920MHz do determine how a particular material and operating frequency of the power signal affected the magnitudes of the following parameters: wavelength (λ) attenuation constant (α), phase constant (β), and the velocity of propagation (v_p). With the exception of the meat, the parameter values increased as the frequency increased and vice versa. It is noted that the inaccurate measurements of the meat may have been attributed to one or more of the following factors: pressing the tip of the probe down on the meat too hard, thereby immersing the probe in blood and shorting it; calibration problems prior to measurements; and inexperienced users operating the probe and network analyzer.

Table 1 – Parameters Affecting Wave Propagation in Biological Tissues

Material	Freq (Mhz)	e'	e''	λ (m/s)	α (Np/m)	β (rad/m)	vp (m/s)
beef	200	77.7483	-1.9592	1.70E-01	4.66E-01	3.69E+01	3.40E+07
beef	440	79.4501	-0.6814	7.65E-02	3.52E-01	8.21E+01	3.37E+07
beef	920	80.2024	2.0396	3.64E-02	2.19E+00	1.73E+02	3.35E+07
oil	200	64.9353	-12.8873	1.85E-01	3.33E+00	3.39E+01	3.70E+07
oil	440	64.989	-8.6202	8.44E-02	4.92E+00	7.45E+01	3.71E+07
oil	915	66.4719	-10.0577	4.01E-02	1.18E+01	1.57E+02	3.67E+07
pudding	200	77.7793	-0.8526	1.70E-01	2.02E-01	3.69E+01	3.40E+07
pudding	440	78.5357	0.6692	7.69E-02	3.48E-01	8.17E+01	3.39E+07
pudding	920	78.6639	2.9895	3.68E-02	3.25E+00	1.71E+02	3.38E+07
saltwater	200	74.8243	0.3536	1.73E-01	8.47E-02	3.62E+01	3.47E+07
saltwater	440	75.0637	0.6424	7.87E-02	3.40E-01	7.98E+01	3.46E+07
saltwater	920	75.7986	1.815	3.75E-02	2.01E+00	1.68E+02	3.45E+07
tankwater	440	77.1122	-0.0881	7.76E-02	4.72E-02	8.09E+01	3.42E+07

Table 2 shows that power attenuated with distance as the EM wave propagated through the materials.

Table 2 – Power vs. Distance

Power (dB)	-31.475	-34.5	-38	-47	-53
Distance (m)	0.03	0.04	0.05	0.07	0.1

What bearing does this have on the lab? What does this mean to me?

As illustrated in Figures 1-4 below, the wave power attenuated rapidly as it propagated over a relatively short distance (0-5cm) through the solid materials before tapering off to substantially zero after z > 6cm. In addition, rapid power loss through the solids occurred over a significantly shorter distance as the wave frequency was increased. Conversely, as shown in Figure 4, power loss occurred significantly more slowly with distance through the saltwater at relatively lower frequencies and very rapidly with distance at relatively higher frequencies. The MATLAB source code used to generate the graphs is documented in the lab notebooks.

NO NEED TO MENTION MATLAB CODE.

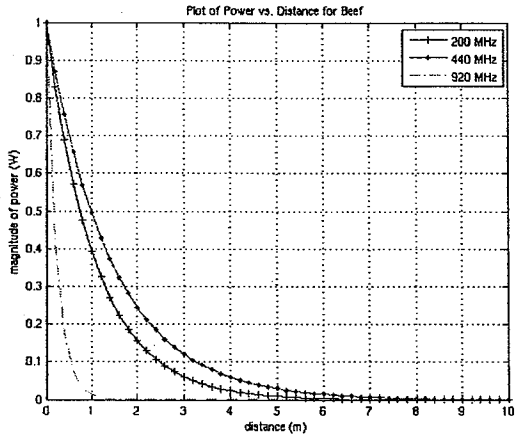

Figure 1 – Plot of Power vs. Distance (beef)

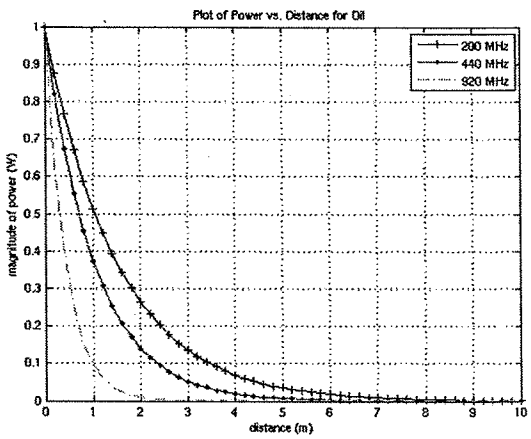

Figure 2 – Plot of Power vs. Distance (oil)

ALWAYS let report stand alone!

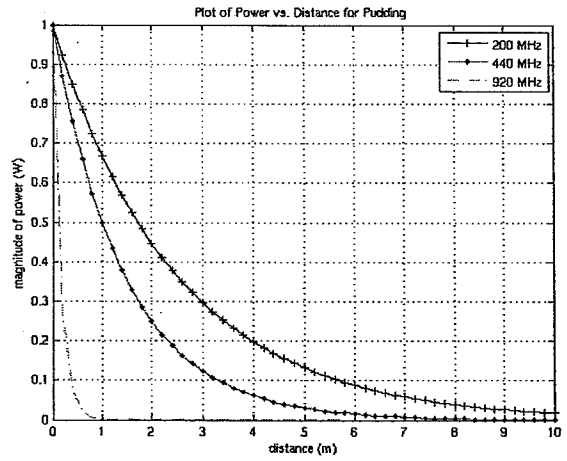

Figure 3 – Plot of Power vs. Distance (pudding)

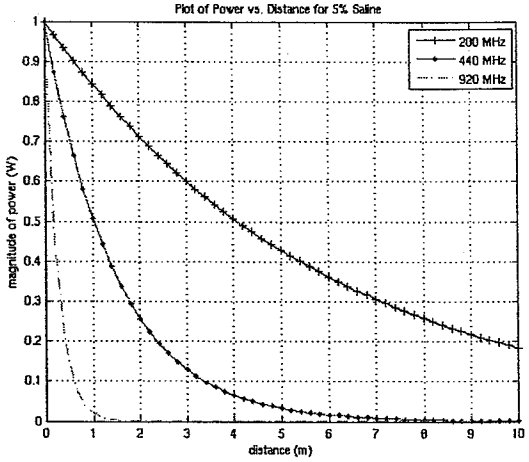

Figure 4 – Plot of Power vs. Distance (saline)

Table 3 depicts calculated values of TL parameters.

Table 3 – Calculated Transmission Line (TL) Parameters Using MATLAB

TL Type	R' (Ω/m)	L' (H/m)	G' (Ω/m)	C' (F/m)	α (Np/m)	β (rad/m)	Vp (m/s)	Zo (Ω)
RG58 coax	3.6996	2.763E-07	4.560E-11	9.085E-11	4.61E-02	3.148E+01	1.996E+08	55.15+.0367j
Twin-lead wire	1.3148	3.860E-07	3.264E-04	6.503E-11	2.11E-02	3.148E+01	1.996E+08	77.04+.0099j

What does this table mean to me?
Why do I care about TL parameters?

Table 4 shows the capacitance measured for various lengths of transmission lines. As shown, the longer the cable, the higher the capacitance thereof. It is inferred that the longer cables had more transmission line effects than the smaller cables.

Table 4 – Measured Transmission Line (TL) Parameters Using a Capacitance Meter

	Lamp Cords (Twin-Lead)				RG-58 Coax		RG-59 Coax		
Capacitance (pF)	10.7	22.6	76.7	156.6	643	735	67.8	130.4	195
Length (ft)	0.0425	0.194	2.917	6.883	21.583	24.583	3.083	6.125	9.167
Length (m)	0.013	0.059	0.889	2.098	6.578	7.493	0.940	1.867	2.794
C' (pF/m)		65.183	66.097		100.612		67.515	69.672	
Average C' (pF/m)		65.640			100.612		68.593		
Prelab C' (pF/m)		64.94			90.72		N/A		
% Error of C'		1.07%			9.83%		N/A		

Table 5 shows a comparison of the capacitance of open-air twin-lead versus buried twin-lead. It was observed that the capacitance of the cables buried in sand was higher than the capacitance of the cables prior to being buried in the sand. Further, the capacitance increased by a higher percentage with increasing length of the cables. This may be attributed to the dielectric constant of sand being higher than that of air.

Table 5 – Transmission Line (TL) Capacitance [twin-lead (in air) vs. twin-lead (in sand)]

Parameter	**Lamp Cords (Twin-Lead)**		
Capacitance (pF) - in air	22.6	76.7	156.6
Capacitance (pF) - in sand	25.4	96.9	206
% Difference of C	12.39%	26.34%	31.55%

Figure 5 below depicts a TDR-generated graph of normalized voltage of an electromagnetic wave at a point in a short-circuited transmission line. The maximum voltage amplitude of 1.5 V varied slightly from the predicted value of approximately 2.0 V. This variation may have been caused by the internal impedance of the TDR itself, as its reflection coefficient is not matched ($\Gamma = 0$) with the transmission line. Graphs for other terminations were recorded in the lab notebook.

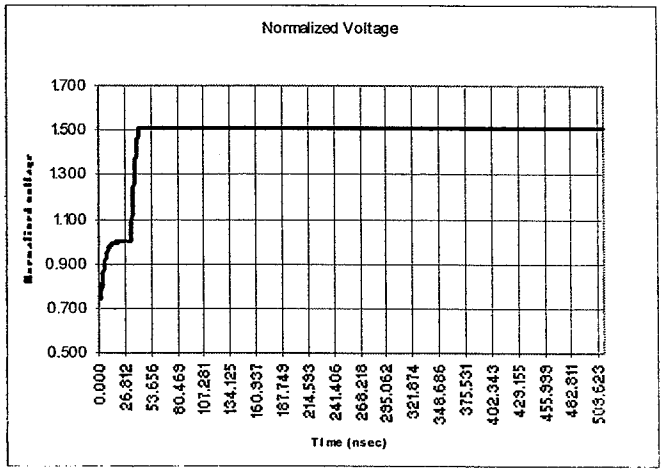

Figure 5 – TDR Graph of RG59 Coaxial Line with $Z_L \approx 0$

As shown in Table 6 below, the Smith Chart calculations of the distance and stub length varied from the values we measured. Based on the calculated values, the impedance mismatch was not completely eliminated. So we used smaller values to obtain a match. A match was successfully obtained with a 2.1cm stub positioned approximately 6.5cm from the antenna, and positioned substantially normal to the main microstrip. A reason for the variances may be attributed to potential errors with using the Smith Chart.

Table 6 – Dimensions of Single Stub Matching Network

	Measured (cm)	Calculated (cm)	Delta (%)
Distance of Stub from Load	**6.5**	**7.5**	**15.0%**
Stub Length	**2.1**	**3.4**	**62.0%**

Table 7 below shows a measured amount of an electric signal that was reflected back from the antenna at 420MHz, 440MHz, and 460MHz, respectfully. As shown, the value of approximately 0.1 mm at 440MHz was relatively low. This value corresponded to a -19.9dB value (as shown in a figure that is in the lab notebooks) that was very close to expected value of at least -20dB. It is concluded that our antenna network was a good match. However, it is ideal for S11 to be zero or otherwise very small. For the ideal case, there would be no signal reflections.

Table 7 – Magnitude of Reflection Coefficient (S11) vs. Frequency

Frequency (MHz)	420	440	460
Magnitude of S11 (mm)	0.216	0.101	0.396

Figure 6 below depicts a plot of the antenna's normalized impedance at a frequency of 440MHz. Its de-normalized impedance value of **42.1+j4.95Ω** slightly varied from an expected value of **36.5 +j0Ω.**

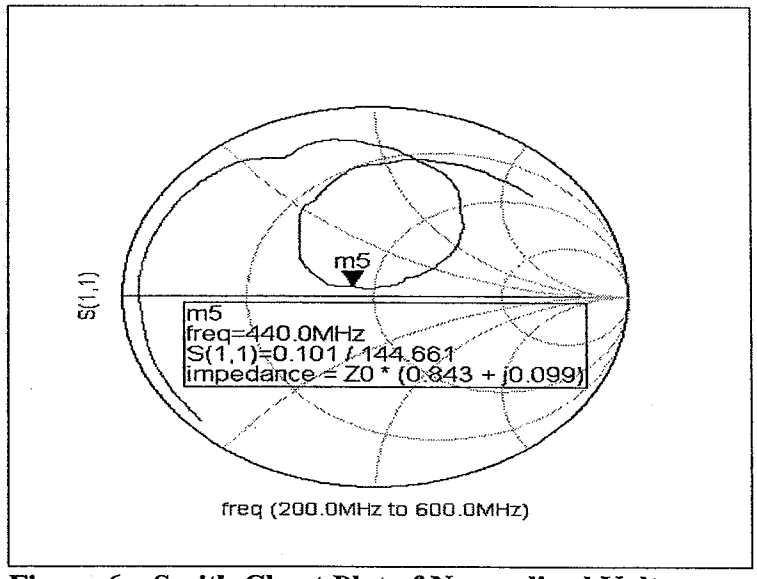

Figure 6 – Smith Chart Plot of Normalized Voltage vs. Time

It was concluded that this slight variation occurred due to the following factors causing the analyzer's reflection coefficient (S11) to be mismatched with the 50Ω line. This mismatch may be caused by the following factors: the internal source impedance of the analyzer; the sensitivity of the network analyzer associated with measurements being taken too close to the analyzer; and imperfect properties of the 50Ω line itself.

In addition to the measurements documented in this report, the following measurements were recorded in the lab notebooks: dimensions of the 50Ω line; power reflected at 420MHz, 440MHz, and 460MHz, and magnitude of S11 at 420MHz, 440MHz, and 460MHz.

Figure 7 below shows the predicted state of a voltage wave propagating through air, using finite-difference-time-domain (FDTD) numerical methods of solving Telegrapher's equations. As shown, the wave dampens out after propagating, through a lossless medium, approximately 60m from its source.

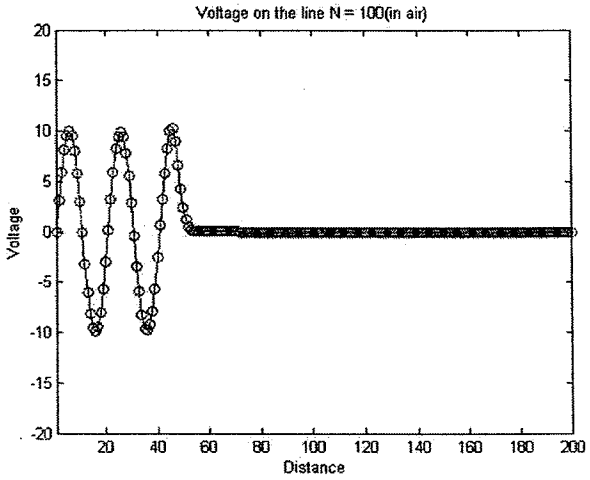

Figure 7 – Voltage on TL in Air (100 time steps)

Figure 8 below shows the predicted state of a voltage wave propagating through seawater, using FDTD numerical methods of solving Telegrapher's equations. Unlike air, seawater is a lossy material as it has a conductivity value greater than zero. The wave dampens out after propagating approximately 25m from its source, significantly quicker that that of air.

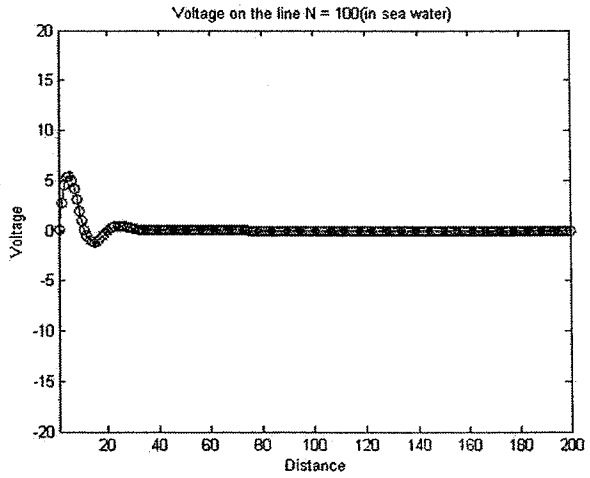

Figure 8 – Voltage on TL in Seawater (100 time steps)

Figure 9 below relates the magnetic field intensity changes with distance. As shown, the intensity of the magnetic field decreases linearly with distance as the EM wave propagates away from its source (e.g., a rod having a cylindrical current distribution).

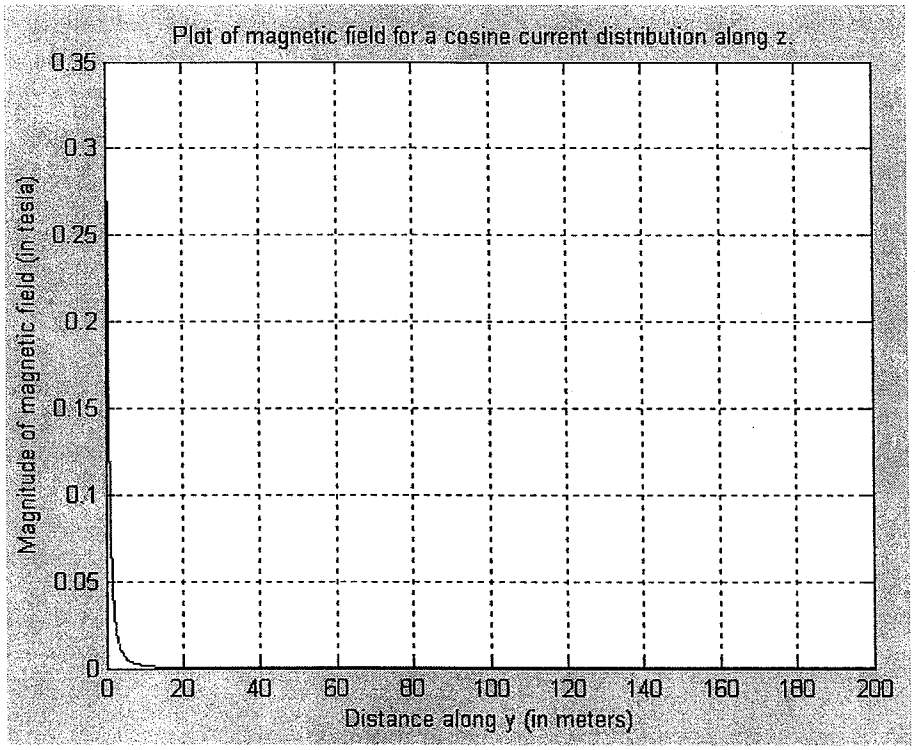

Figure 9 – Plot of Magnetic Field Strength vs. Distance

Figure 10 depicts the transmitter as a component of the FSK system. As shown, the transmitter consists of a control circuitry that controls operation of the transmitter, a voltage-controlled oscillator (VCO) the generates input signals, and a dipole antenna configured to be submerged in the human tissue simulant.

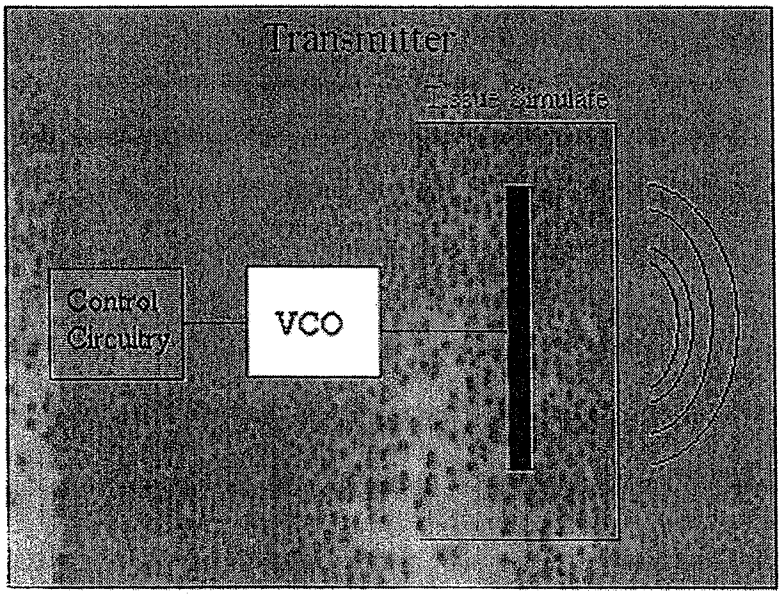

Figure 10 – Transmitter

Figure 11 depicts the receiver as a component of the FSK system. As shown, the receiver consists of a radio-frequency (RF) amplifier; a power splitter that splits an input signal into two output signals; a band pass filter that passes the two signals at 420MHz and 460MHz; and a decision circuit that determines the signal frequency is being sent. The receiver also includes the single-stub matching network with a monopole antenna attached thereto.

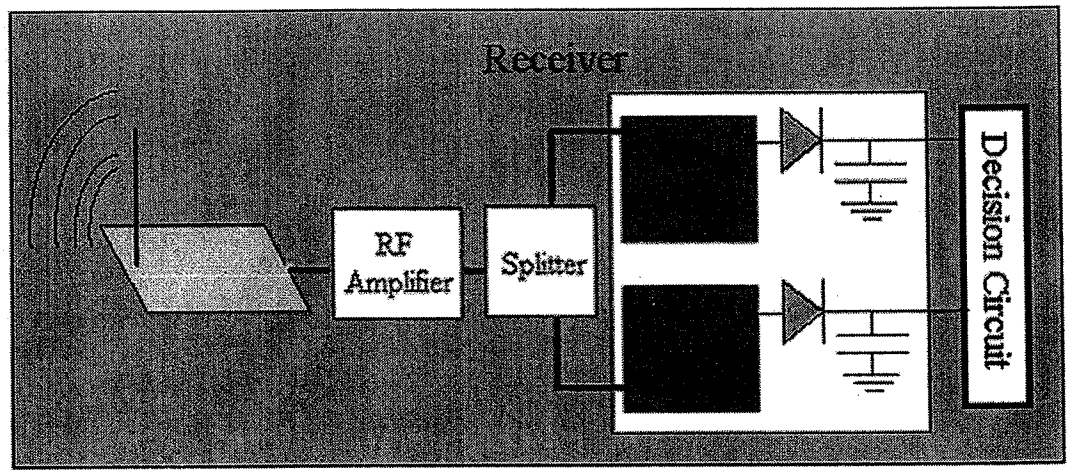

Figure 11 – Receiver

Table 9 gives the reflection coefficients for S11 in two different materials. In order to properly calculate the appropriate numbers for total results the reflections from the respective waves need to be obtained and included in the measurements and also in the calculations for the system.

Table 9 - Reflection Coefficient (S11) of Receiver (1m from Transmitter)

Frequency (MHz)	420	440	460
S11 (in air)	-3.7 dB	-5.0 dB	-5.5 dB
S11 (in simulant)	-15.8 dB	-16.1 dB	-13.2 dB

Table 10 below relates the intensity of power transmitted with orientation of the transmitting (dipole) antenna relative to the receiving (monopole) antenna. As shown, maximum power is transmitted when the transmitting dipole antenna is parallel to the receiving monopole antenna, based on the given distance. Likewise, the minimum power is transmitted when the transmitting antenna is positioned perpendicular to receiving antenna.

Table 10 – Transmission Coefficient (S21) of Transmitter (1m from Receiver)

	420	440	460
S21 (transmitter parallel to receiver)	-42.5dB	-59.0dB	-62.0dB
S21 (transmitter normal to receiver)	-48.8dB	-50.3dB	-61.9dB

As shown in Table 11 below, the receiver's sensitivity was measured to be -13dB in step one, so we are calculating the maximum distance in air to be 33 cm for successful transmission. This matches the measured values in Table 4.

Table 11 - Power Link Budget Program Output

	Distance between Transmitter & Receiver (in air)	**Total Power Delivered to Receiver**
No Amplifier coupled to Receiver	17 cm	-8.0251 dB
One Amplifier coupled to Receiver	33 cm	-13.7864 dB

Your results section should tell a story of what you got and why it's important. You shouldn't just lay out all of the figures and tables you can find and comment on each one. Your figures and tables should support your text, not the other way around.

4.0 DISCUSSION:

During the first experiment, the beef represented 2/3 human muscle, the oil represented fatty tissue, the saline solution represented the salty liquids in the human body, and the pudding represented nerve tissue, cartilage, and other body tissues. The attenuation caused in the chest cavity of a human being can be roughly represented using 2/3 muscle mass. Careful measurements have been done to ascertain dielectric constants for biological tissues [7]. These measurements can be used to calculate the amount of power required initially to send a certain amount of power to the surface of a material (such as the chest cavity).

It was observed, as shown in Section 3.0, Table 1 and Figures 1-4, that power attenuation gets larger with increasing conductivity of a material. In addition, as the operating frequency of a signal increases, the smaller skin depth results in greater attenuation. The parts of the human body that the substances would tend to act most like are the small amount of muscle on the inner layer of skin, the skin itself, and the surrounding fatty tissue.

The predicted attenuation values were relatively close to the measured values of attenuation at an operating frequency of 440 MHz, but deviated at the higher frequency. In addition, the measured values differed from the measured values obtained from other personnel in the lab, particularly the third value of α. The differences between the calculated and predicted values of α may be attributed to the following factors: differences in calibration of the probe; inherent error tolerances of the lab equipment (e.g., probe, network analyzer, antennas); differences in personnel experience and/or method of employing the probe to take measurements of the dielectrics; the experimental permittivity (ε) and permeability (μ) values of dielectric materials as listed in Final Technical Report [2] that affect the predicted values of α.

The dielectric regions in a cardiac pacemaker system inside the body include layers of human skin, muscle, fatty tissue, etc., each having its own values of ε, μ, conductivity (σ) that effect its ability to attenuate power of an EM wave propagating through them, as learned during the pre-lab when measuring the dielectric properties of biological materials listed in the Laboratory Handout [1] and the Dielectric Properties of Biological Tissues Article [3]. Outside the body, it's the distance between the pacemaker's electrodes/probes from the surface of the human body that affects the power attenuation of an EM wave, as learned during this experiment.

Other sources of power loss in a cardiac pacemaker system includes, but is not limited to: differences in weight, build, muscle/fat distribution of various people employing the system; error tolerances/manufactured imperfections of each individual pacemaker; differences of internal impedances of the probes/electrodes, antenna, and other components of the pacemaker system; differences in internal impedances of the human body; differences in distance between a person's body surface and his or her heart; etc.

Based on the measurements taken during the second experiment, as shown in Section 3.0, Table 4, as the length of a line increases the capacitance of the line increases as well. For the RG-59 coaxial cable: the lengths of 3.083 ft, 6.125 ft, and 9.167 ft correspond to 67.8 pF, 130.4 pF, and 195 pF respectively. For the twin-lead cable: 0.194 ft, 2.917 ft, and 6.883 ft correspond to 22.6 pF, 76.7 pF, and 156.6 pF respectively.

In addition, as shown in Section 3.0, Table 5, it was observed that the capacitance of the cables buried in sand was higher than the capacitance of the cables prior to being buried in the sand. More, the

capacitance increased by a higher percentage with increasing length of the cables. This may be attributed to the dielectric constant of sand is higher than the dielectric constant of sand.

Burying the twin-lead cable increased the capacitance. Special care was taken to ensure that the entire length of line except about two inches was buried and this resulted in an increasing percentage difference for each length. The 0.194 ft, 2.917 ft, and 6.883 ft cables increased by 12.39%, 26.34%, and 31.55% respectively after burial, as shown in Section 3.0, Table 5. More experimentation is needed, but this appears to be an exponential growth. Capacitance is a good general measure, but it lacks precision for locating faults since it depends on its environment for a numerical value.

Further in this lab, various transmission line terminations were measured using time domain reflectometry (TDR). The capacitance of different lengths of transmission lines was measured using a capacitance meter; the capacitance of an open-air transmission line was compared to that of a buried transmission line with the same characteristic geometry.

When used in a cardiac pacemaker application, the effects of reflections on a discontinuity in a transmission line can be very useful for locating faults and determining the impedance of the load termination of a system. Using TDR to determine the load termination of a system can locate precisely where a fault lies in a wire. If the fault is completely open, it will look capacitive, otherwise tandem lines will be present in the line. TDR is a superior method for locating faults in a line.

The third experiment involved the design of a single-stub matching network, such that maximum power can be delivered to the receiver. During this lab impedances of transmission lines and antenna were measured using a calibrated HP8720C Network Analyzer. The analyzer was also used to measure the magnitude of power delivered from a source of a load; and the amount of power reflected from the source to load. The measurements were crucial in the design of a stub line that was coupled to the main microstrip line, and used to help in matching the impedances of a second line and antenna.

As shown in Section 3.0, Table 6, it was observed that the calculated stub length of 3.4cm was approximately 62% larger that the measured length of 2.1cm. In addition, the stub was calculated to be approximately a distance of 7.5cm from the antenna. This distance calculation was 15% larger that the measured distance of 6.5cm. The differences between the calculated and measured values may be attributed to the use of an imperfect Smith Chart to calculate the values vs. using an actual distance measuring device.

More, as documented in Section 3.0, Table 7 it may be inferred that the magnitude S11 increased with frequency with the exception of 440MHz. The S11 values of 0.216mm, 0.101mm, and 0.396mm, respectfully, corresponded to frequencies of 420MHz, 440MHz, and 460MHz, respectfully. Given the fact that only three measurement values were recorded in the experiment, more experimentation is needed to support a conclusion of such trend. Further, the analyzer was very sensitive apparatus, such that any abrupt movement of the 50Ω coax can result in unrepresentative measurements.

The fourth stage of the experiment involved the application of numerical analysis and MATLAB to employ the numerically solve Telegrapher's first-order differential equations (ODEs) relating the rate of change of a voltage/current wave with respect to space and time. In particular, with the Telegrapher's equations was converted to FDTD difference equations for current and voltage. This enabled MATLAB to be employed to solve the equations and predict the future changes of current and voltage as the waves propagate in space over a period of time. MATLAB was very helpful, as Telegrapher's ODEs can be

solved analytically, but the analytical method proved difficult when predicting future behaviour of EM waves. With the understanding that magnetic field intensity decreases with distance, helped in the awareness that it also results in power attenuation the farther the pacemaker is implanted into human tissue.

As shown in Section 3.0, Figures 9 and 10, over time the signal decreases significantly more rapidly in seawater (lossy medium) than in air (lossless medium) over distance and time. This experiment was important as understanding of this information is needed, during the design of the system, to determine how fast power attenuation occurs according to the dielectric properties of the human simulant. This has an effect on how far to implant the cardiac pacemaker into a person's body place, whereby the signal can still be transmitted to the external receiver with minimal loss.

The fifth stage of the experiment again involved the application of numerical analysis and MATLAB to employ the Trapezoidal method to numerically compute Biot-Savart's integral in order to how magnetic field intensity, generated by the electrical signal, changes with distance as the signal propagates away from its power source. As shown in Section 3.0, Figure 9, the magnetic field intensity decreases linearly with increasing distance from its source (e.g. a current distribution of a cylindrical rod). MATLAB was very helpful, as the Biot-Savart's integral would be very difficult task to compute analytically. With the understanding that magnetic field intensity decreases with distance, helped in the awareness that power attenuation increases the farther the pacemaker is implanted into human tissue.

The sixth and final experiment involved the design and testing of a prototype FSK system, as shown in Section 3.0, Figures 10 and 11. While measuring he distances between the transmitter and receiver, it was observed that multi-path communications had a profound effect on the operability of the system. There were numerous reflections that formed standing waves showing power maximums and power minimums. As a result, the amount of power gain at the receiver varied with distance. There were distances where power gain was at a minimum and at a maximum. The distance measurements are documented in the lab notebooks.

In addition, waiting in the same location in time appears to provide a constant power gain unless interference is introduced into the system. Waving hands by the antenna and walking around in front of the antenna changed the signal. This is probably due to changing the distances of the multi-path reflections that add together differently.

Try to relate each lab more to the bigger picture - You had good explanation of each one, but don't forget what that really means. Especially concluding paragraph

5.0 CONCLUSIONS AND RECOMMENDATIONS:

During the first experiment, the dielectric constants for various materials were measured and calculated. In particular, the dielectric constants for beef, oil, 5% saline solution, and pudding mixture were measured using the network analyzer and the attenuation constant calculated and plotted. Each of these materials represented a biological tissue found in the chest cavity including muscle, nerves, water, and fat. A trend shown was that an increase in frequency corresponded to an increase in attenuation. Using a lower frequency will allow a pacemaker to send a signal that will attenuate significantly less than a high frequency signal. Therefore, a lower frequency signal is more likely to make it through the chest cavity to the electronic equipment outside of the body.

These considerations will need to be part of the design and analysis of a pacemaker system. Otherwise, the pacemaker may not provide enough power to the signal so that it reaches the air or reader outside of the chest cavity. Other factors may also affect attenuation like bone, internal reflections, and possibly more. All these things will have to be measured before the pacemaker is ready for implantation into a human being.

During the second experiment, it was shown that using the network analyzer to match impedances of the source(s), line(s), and load(s) can help in the virtual elimination of wave reflections and standing waves in order to maximize the magnitude of power that may be delivered through a transmission medium to a load. This would optimize the design of a pacemaker that can transmit maximum power, resulting in a working communication between the pacemaker and the reader.

Applying numerical analysis with MATLAB simulations helped to understand how changes in magnetic field intensity and future changes in a power signal over distance in space and time relate to the magnitude of power attenuation that may occur. Power transmitted by the pacemaker through lossy materials (e.g., human tissue) can affect the system's ability to deliver critical medical information to medical staff monitoring patients with cardiac pacemakers implanted in their bodies.

The final experiment culminated in the actual design of a prototype FSK system. While designing the system, it was discovered that using an amplifier in the simulant was sufficient to produce a signal strong enough to be transmitted to the receiver. The signal operating frequency of 440 MHz is also sufficient to carry the signal through the simulant that acted as the body for a patient who need the pace maker. The total power using the link budget of the receiver was calculated to be -14dB. In the bigger picture, the design of a power link budget has proven to be a successful and an accurate way to measure the power required for a wireless communication system to operate. It will likely be successful if it is implemented in the pacemaker communication system.

In conclusion, the processes of this experiment helped to design a system that would allow for wireless pacemaker to be placed inside the human body. The pacemaker will use a transmitter to send data to an external receiver that is connected to a PC which processes the data to monitor the patient's health. Measuring the dielectric properties of substances similar to the fat, skin, and muscle of the patient allowed us to determine the attenuation of a signal passing through these types of material. It was shown that construction of such a device is feasible, and a power link budget was calculated for an external implementation.

REFERENCES:

[1] Dr. C. Furse, ECE 3300 Lab 1 Procedures, *Dielectric Properties of Materials*, Sep 2007

[2] Dr. C. Furse, ECE 3300 Lab 2 Procedures, *Transmission Lines & Time-Domain Reflectometry*, Sep 2007

[3] Dr. C. Furse, ECE 3300 Lab 3 Procedures, *Monopole Antenna & Single Stub Matching Network*, Sep 2007

[4] Dr. C. Furse, ECE 3300 Lab 4 Procedures, *Telegrapher's Equation Using FDTD Method*, Sep 2007

[5] Dr. C. Furse, ECE 3300 Lab 5 Procedures, *Numerical Integration & Biot-Savart's Law*, Sep 2007

[6] Dr. C. Furse, ECE 3300 Lab 6 Procedures, *FSK Communication System*, Sep 2007

[7] S. Gabriel, R. Lau, C. Gabriel, "The Dielectric Properties of Biological Tissues II: Measurements in the Frequency Range 10 Hz – 20 GHz," *Phys. Med. Biol.*, Vol 41, pp. 2251-2269, 1996.

[8] C. Gabriel, "Compilation of the dielectric properties of body tissues at RF and microwave frequencies," *Final Technical Report*, Occupational and Environmental Health Directorate Radiofrequency Radiation Division, Brooks Air Force Base, TX, 1996.

[9] S. Wentworth, "Applied Electromagnetics – Early Transmission Line Approach", John Wiley & Sons, Inc., 2007.